JOURNAL OF APPLIED POLYMER SCIENCE VOL. 21, 3003–3022 (1977)

Melt Spinning of Isotactic Polypropylene: Structure Development and Relationship to Mechanical Properties

HARI P. NADELLA, HELEN M. HENSON,* JOSEPH E. SPRUIELL, and JAMES L. WHITE, *Department of Chemical and Metallurgical Engineering, The University of Tennessee, Knoxville, Tennessee 37916*

Synopsis

An extensive experimental study of structure development during the melt spinning of polypropylene and in as-spun polypropylene filaments is reported. Five polymers representing different molecular weights and polymerization methods were studied. WAXS, SAXS, and birefringence measurements were used to characterize the structure of the filaments. Spinning through air gives rise to monoclinic crystalline structures and spinning into cold water, the paracrystalline smectic form. Both crystalline and amorphous orientation factors were found to correlate with spinline stress for the different polymers studied. Mechanical properties of as-spun fibers such as modulus, yield strength, tensile strength, and elongation to break also correlate with spinline stress.

INTRODUCTION

Isotactic polypropylene is an important commercial plastic, film, and synthetic fiber. As a fiber, it may exhibit a wide variety of mechanical properties. By suitable processing, it can be used to produce very high modulus and tensile strength fibers[1] or microporous fibers (and films) with large elastic recovery.[2–5] These facts make basic studies of the development of structure and properties of polypropylene fibers as a function of melt-spinning conditions of considerable interest.

The pioneering study of the melt spinning of polypropylene is that of Sheehan and Cole.[1] These authors show that monoclinic polypropylene is produced under normal air quenching conditions, but quenching in cold water produces a paracrystalline smectic structure. Hot drawing of fibers, especially smectic fibers, spun at low take-up velocities yields very high strength fibers. Katayama, Amano, and Nakamura[6] have carried out on-line wide-angle x-ray diffraction and birefringence studies on a spinline and followed the development of crystallinity and orientation. More recently, structure development during melt spinning of polypropylene has been investigated by Fung, Orlando, and Carr,[7] Kitao, Ohya, Furukawa, and Yamashita,[8] Anderson and Carr,[9] Henson and Spruiell,[10] Spruiell and White,[11,12] and Ishizuka and Koyama.[13] Kitao et al. have analyzed the development of orientation in terms of Hermans-Stein-Wilchin-

* Present address: Union Carbide Nuclear Division, Oak Ridge, Tennessee 37830.

sky[11,14–17] orientation factors. Spruiell et al.[10–12] have carried out on-line x-ray diffraction and birefringence measurements, quantitatively determined spinline crystallization kinetics, and shown that orientation factors depend upon spinline stress independent of temperature. Polypropylene exhibits unique bimodal orientation when crystallized under stress.[9,10,18] Interpretation of the possible implication and mechanisms of this bimodal orientation have been given by Clark,[19] Anderson and Carr,[9] Spruiell et al.,[10,12] and Clark and Spruiell.[20]

In this paper, we explore the relative behavior of a series of polypropylenes of varying molecular weight and produced by different catalyst systems. This paper continues our studies of structure development during melt spinning.[10–12,21–24] It is also part of an extensive study of the processing of polypropylene in our laboratories which include rheological as well as structure development studies.

EXPERIMENTAL

Materials

Five different polypropylenes with varying levels of molecular weight were studied. Their basic characteristics are summarized in Table I, together with a code naming system. Three of the polymers were highly isotactic Hercules Profax, and two were in the Tennessee Eastman Tenite series. The latter also possess a high level of tacticity, but, perhaps, not quite as high as the Profax polymers. Other possible differences include molecular weight distribution. In the present study, these effects were not fully investigated. A more detailed study of molecular weight distribution effects is underway and will be published at a later date.

The intrinsic viscosities given in Table I were determined at 137°C in decalin and converted to molecular weight using the expression[25]

$$M = ([\eta] \times 10^4)^{1.25} \tag{1}$$

TABLE I
As-Received Polymer Properties

Manufacturer and commercial code	Melt index, g/min	Our code name	Intrinsic viscosity, dl/g	Weight-average molecular weight	Tacticity
Hercules Profax 6823	0.42	H-0042	3.21 (3.25, 3.30[a])	4.30×10^5	very high
Hercules Profax 6423	6.6	H-0660	2.26	2.77×10^5	very high
Hercules Profax 6323	12.0	H-1200	1.99	2.36×10^5	very high
Tennessee Eastman Tenite 4241	9.00	T-0900	2.01	2.39×10^5	high
Tennessee Eastman Tenite 4221	2.55	T-0255	2.71	3.48×10^5	high

[a] Courtesy of Hercules, Inc.

Melt Spinning

The polypropylenes were melt spun from a Fourné Associates screw extruder and spinning head. The extruder had a 13-mm diameter screw. Constant throughput was maintained by a Zenith gear pump. The spinneret capillary was 0.381 cm long and 0.0762 cm in diameter.

The extrusion temperature was kept constant at 230°C except for H-0660; in this case, filaments were also spun with extrusion temperatures of 200° and 260°C. The polymers, with the exception of H-0042, were extruded at a rate of 2.1 g/min. The H-0042 exhibited extrudate distortion[26,27] under these conditions; to eliminate this, the extrusion rate was reduced to 0.5 g/min. The filaments were normally melt spun through stagnant air at approximately 25°C and were passed around a 3-in. diameter, constant-speed feed roll placed 10 feet from the spinneret. After leaving the feed roll, the filaments were taken up on a Leesona 955 constant-tension winder. Filaments were taken up at speeds of 50, 100, 200, 400, and 550 m/min whenever this was feasible. A Rothschild tensiometer with a 10-g measuring range was used to measure the fiber tension.

In an attempt to produce smectic spun filaments as described by Sheehan and Cole,[1] some H-0660 polymer was spun into a water bath at 9°C placed 9 in. from the spinneret. These filaments were taken up at speeds varying from 25 to 300 m/min.

Wide-Angle X-Ray Diffraction and Crystalline Orientation

Wide-angle x-ray diffraction patterns of the spun filaments were made using a flat plate-type camera and nickel-filtered CuK_α radiation. These patterns were used to determine the crystalline form present and the qualitative features of the orientation.

On-line WAXS measurements on the spinline were made using Rigaku-General Electric rotating-anode generator. This is the apparatus developed by Dees and Spruiell[22] and used by them on high-density polyethylene. Parts of these on-line results for polypropylene have been reported by Spruiell and White.[11,12] The crystalline fraction X was determined from microdensitometer scans made on the WAXS patterns. The relative intensity in the crystalline reflections compared to the amorphous halo was used to compute a crystalline index. The data were normalized by considering density values of X on spun filaments as correct.

Quantitative studies of crystalline orientation were made by measuring the intensity distributions around the Debye rings with a General Electric x-ray diffractometer equipped with a single crystal orienter and an ORTEC counting system. The 040 and 110 monoclinic reflections were measured and used to compute Hermans–Stein crystalline orientation factors.[12,15–17] These factors indicate the orientation of the crystallographic axes with respect to the fiber axis. They are defined in such a way that the orientation factor is unity for a crystallographic axis which is parallel to the fiber axis, equal to −0.5 if the axis is aligned perpendicular to the fiber axis and zero if the axis is distributed randomly. The orientation factors are given by

$$f_j = (\overline{3\cos^2\phi_{j,z}} - 1)/2 \tag{2}$$

where $\overline{\cos^2\phi_{j,z}}$ is the average value of the cosine squared of the angle between the fiber axis and the j-crystallographic axis ($j = a$, b, or c). Assuming rotational symmetry about the fiber axis,

$$\overline{\cos^2\phi_{j,z}} = \frac{\int_0^{\pi/2} I_{hkl}(\phi_{j,z}) \cos^2\phi_{j,z} \sin \phi_{j,z} d\phi_{j,z}}{\int_0^{\pi/2} I_{hkl}(\phi_{j,z}) \sin \phi_{j,z} d\phi_{j,z}} \tag{3}$$

where $I_{hkl}(\phi_{j,z})$ is the intensity diffracted from the (hkl) planes which are normal to the j-crystallographic axis.

Using eqs. (2) and (3), the value of f_b was computed from the intensity distribution in the 040 reflection. In monoclinic polypropylenes, the chains are helices whose axes lie along the c-crystallographic axis. There is no convenient set of diffraction planes perpendicular to the c-axis, and the method of Wilchinsky[16,17] was used to compute f_c. He has shown that for monoclinic polypropylene,

$$\overline{\cos^2\phi_{c,z}} = 1 - 1.099\,\overline{\cos^2\phi_{110,z}} - 0.901\,\overline{\cos^2\phi_{040,z}} \tag{4}$$

where $\cos^2\phi_{110,z}$ and $\cos^2\phi_{040,z}$ are obtained from intensity measurements on the 110 and 040 reflections and eq. (3).

For orthogonal crystal axes,[15]

$$f_a + f_b + f_c = 0 \tag{5}$$

In the case of monoclinic polypropylene, the a-axis is not perpendicular to the c-axis, but it makes an angle of 99.3°. In this case, it is convenient to define an a'-axis which is not a true crystallographic axis but is perpendicular to both the b- and c-crystallographic axes and whose orientation factor can be determined from eq. (5) and the values of f_b and f_c.

Small Angle X-Ray Diffraction

Small-angle x-ray diffraction (SAXS) patterns were obtained on selected fiber samples using a modified Kiessig camera with pinhole collimation. The camera was mounted on a Rigaku-General Electric rotating anode x-ray generator. The patterns were obtained under vacuum conditions, and a custom-made collimator was used. The resolution was about 400 Å.

Density

The crystalline fraction in fibers (determined from WAXS patterns to be monoclinic) were measured in a water–isopropyl alcohol gradient density column at 23.2°C. The column was constructed as described by Tung and Taylor.[29] The samples were allowed approximately 12 hr to seek their level of displacement. Specific volumes $\overline{V}$ were converted to crystalline fraction X through the expression

$$X = \frac{\overline{V}_a - \overline{V}}{\overline{V}_a - \overline{V}_c} \tag{6}$$

where $\overline{V}_c$ and $\overline{V}_a$, the specific volumes of crystalline and amorphous polypropylenes, were obtained from Danusso et al.[30]

Birefringence

The birefringence Δ of the fibers was determined using an Orthoplan polarizing light microscope with a Leitz Berek Compensator. The birefringence of the fiber is the ratio of the measured phase difference to the diameter of the filament. On-line birefringence measurements were made by the same technique with the microscope appropriately mounted so as to observe the running threadline.

Amorphous Orientation

The level of amorphous orientation in the fibers was determined using the theory of Stein and Norris[31] in the manner applied to polypropylene previously by Hoshino et al.[32] and Samuels.[17,33,34] This involves consideration of the relative amorphous and crystalline contributions to the birefringence, calculating the latter and subtracting it out. Specifically, one writes

$$\Delta = f_c X \Delta^0_{\text{cryst}} + f_{\text{amorph}}(1 - X)\Delta^0_{\text{amorph}} + \Delta_{\text{form}} \tag{7}$$

where Δ^0_{cryst} and Δ^0_{amorph} are the intrinsic birefringences of the crystalline and amorphous regions. Δ_{form} is the so-called "form birefringence" [35] and is neglected in the calculations. To calculate f_{amorph}, we use Δ from birefringence measurements, X from density values, and f_c from WAXS measurements. We accept Samuels' results for Δ^0_{cryst} and Δ^0_{amorph}.

Mechanical Properties

The mechanical properties of the melt-spun fibers were measured at room temperature with an Instron tensile tester. Force-versus-elongation curves were obtained at a cross-head speed of 2 in./min using an initial fiber length of 1 in. The tangent modulus, yield strength, tensile strength, and percent elongation to break were measured.

GENERAL SPINNING BEHAVIOR AND STRESS DEVELOPMENT

Certain qualitative features of spinning behavior were apparent. As noted previously, extrudate distortion occurred in the H-0042 at the spinning temperature and flow rate used for all other polymers ($\dot{\gamma}_{w,2.1} \sim 900\ \text{sec}^{-1}$). In order to obtain smooth extrudates, the melt spinning for this specimen was achieved by reducing the flow rate from 2.1 g/min to 0.5 g/min ($\dot{\gamma}_{w,0.5} \sim 210\ \text{sec}^{-1}$).

The Tennessee Eastman polymers could only be spun under limited conditions. With an extrusion temperature of 230°C and an extrusion rate of 2.1 g/min, melt draw ratios V_L/V_0 less than or equal to 62 were achieved. (The polymer grades used in this investigation were not necessarily recommended for fiber spinning by their manufacturers. They were chosen more on the basis of their known differences in behavior than on their ability to be spun.) These polymers exhibited decreasing spinnability with increasing molecular weight.

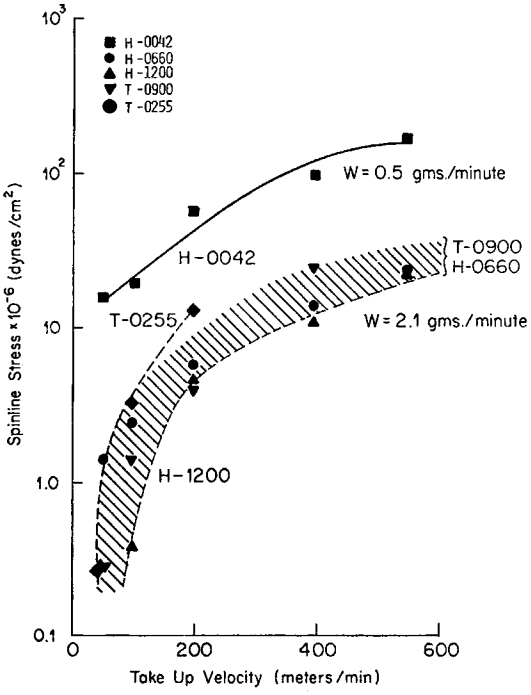

Fig. 1. Effect of take-up velocity on spinline stress of polypropylene fibers. Extrusion temperature is 230°C.

The H-0660 and H-1200 samples could be melt spun at higher take-up speeds and melt draw ratios. Under similar extrusion conditions, samples were spun with $V_L/V_0 = 95$. At the same extrusion rate, higher melt draw ratios could not be examined because of the limitations of our winding apparatus. The H-0042 was drawn down to ratios of 410.

The differences between Hercules and Tennessee Eastman polymers probably could be traced to the fact that the two manufacturers use different catalyst systems in the preparation of the polymers. This may result in differences in tacticity and/or molecular weight distribution. The latter effect may be responsible for the observed differences in spinnability.

The influence of the spinning conditions on the molecular weight of the po-

TABLE II
Characterization of As-Spun Polypropylene Fibers

Sample code	Intrinsic viscosity, dl/g	Weight-average molecular weight	Percent thermal degradation[b]
H-0042	2.50 (2.55[a])	3.14×10^5	27
H-0660	2.24	2.74×10^5	1
H-1200	1.70	1.94×10^5	18
T-0900	1.83	2.13×10^5	11
T-0255	2.33	2.88×10^5	17

[a] Courtesy of Hercules, Inc.
[b] During extrusion.

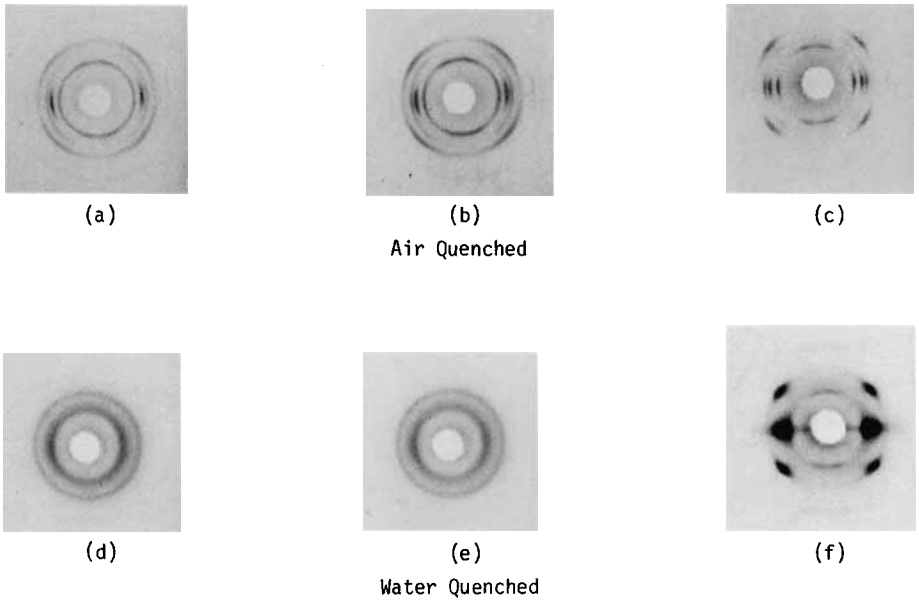

Fig. 2. Effect of take-up velocity and cooling medium on WAXS patterns of H-0660 polypropylene fibers. Extrusion temperature = 230°C. Air quenched: (a) 50 m/min; (b) 200 m/min; (c) 550 m/min. Water quenched: (d) 25 m/min; (e) 100 m/min; (f) 300 m/min.

lypropylenes was assessed from intrinsic viscosity measurements. These results are given in Table II. Degradation due to melt spinning was observed in all the polymers with values ranging from 1% to 27%. The highest degradation (27%) was observed for H-0042, the sample with the highest molecular weight. The molecular weights given in Table II are more significant than those in Table I when considering the structure and properties of the spun filaments.

Figure 1 shows changes of the stress in the spinline with take-up velocity and mass flow rate. The spinline stress was found to increase with the take-up velocity for all the polymers at a specific melt flow rate. The effect of the molecular weight can be observed from the data for samples spun at a melt flow rate of 2.1 g/min. The samples of T-0255 show higher stress levels at a given take-up velocity than the H-1200 samples, and the data on the intermediate molecular weight specimens were scattered between T-0255 and H-1200. Thus, in general, there was a trend toward increasing spinline stress levels with increasing molecular weight. The data also seem to indicate a large effect of melt extrusion rate on the spinline stress. This effect is associated in part with the increased draw-down ratio V_L/V_0 accompanying a decreased extrusion rate through the spinneret and with the increased cooling rate of the smaller diameter filaments. The stress levels in the melt ranged from 0.3×10^6 dynes/cm^2 to 170.0×10^6 dynes/cm^2.

STRUCTURE DEVELOPMENT DURING MELT SPINNING

Qualitative Features

Depending on the threadline cooling rates, the spun filaments of polypropylene were either smectic (paracrystalline) or highly crystalline. The crystalline form

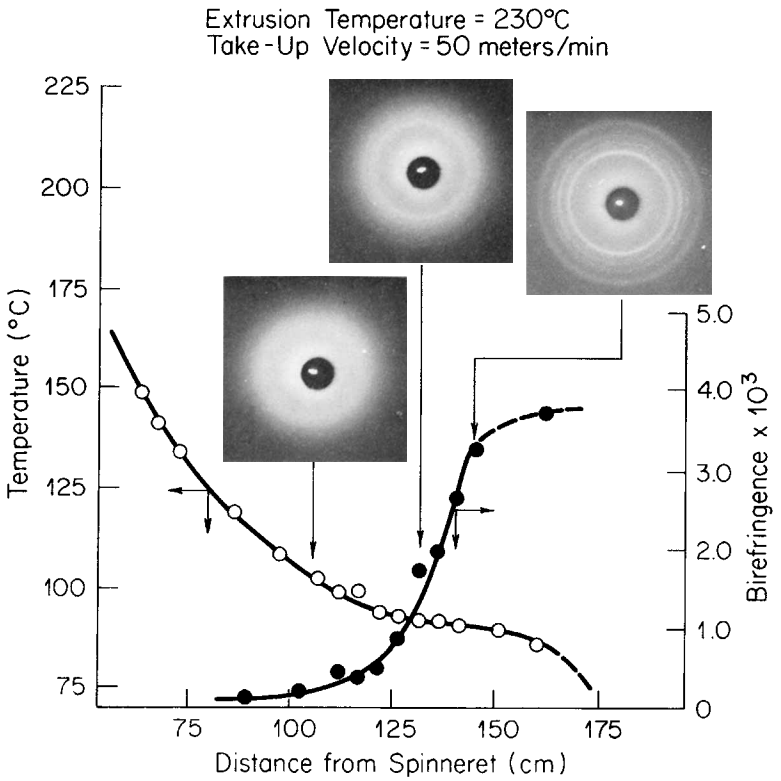

Fig. 3. On-line WAXS patterns, temperature and birefringence profiles for melt-spun H-0660 polypropylene filament.

is the monoclinic α-form. In the present study, it is primarily the highly crystalline monoclinic filaments that were produced. The smectic form occurred only when rapid cooling rates were achieved by quenching the molten threadline into water.

Figure 2 shows WAXS patterns of H-0660 filaments spun either into ambient air or into water at 9°C. The effect of increasing take-up velocity (and spinline stress) is also shown. All filaments were spun with an extrusion temperature of 230°C. It can be seen in Figure 2(a)–2(c) that the samples are highly crystalline and the c-axis orientation is increasing with take-up velocity. For the smectic form in Figure 2(d)–2(f), there is a transformation in crystal structure from an unoriented paracrystalline to highly oriented partially monoclinic type with increasing take-up velocity.

For filaments spun into ambient air, crystallization to the monoclinic form occurs in the threadline. This fact is easily demonstrated with on-line measurements as shown in Figure 3. Here, x-ray patterns made on a running filament at different distances from the spinneret are shown in relation to a temperature and birefringence profile for the same run. A hold in the temperature profile occurs as crystallization begins due to the release of the latent heat of crystallization. During crystallization the birefringence rises rapidly, eventually approaching the birefringence of the as-spun filament.

The effect of spinning temperature on the WAXS pattern is shown in Figure 4 for the H-0660 polymer. Increasing the spinning temperature with other

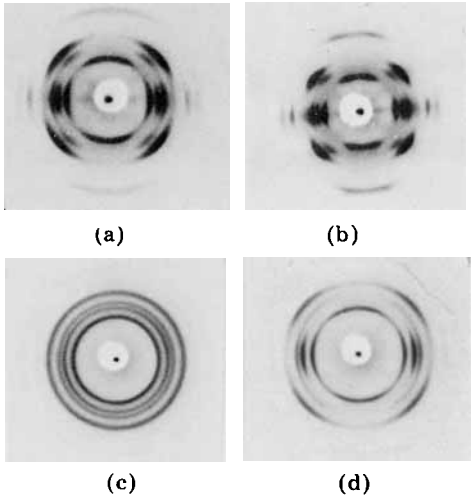

Fig. 4. Variation of the WAXS patterns for H-0660 polymer with extrusion temperature T_E and take-up velocity V_L: (a) T_E = 200°C, V_L = 50 m/min; (b) T_E = 200°C, V_L = 550 m/min; (c) T_E = 260°C, V_L = 50 m/min; (d) T_E = 260°C, V_L = 550 m/min.

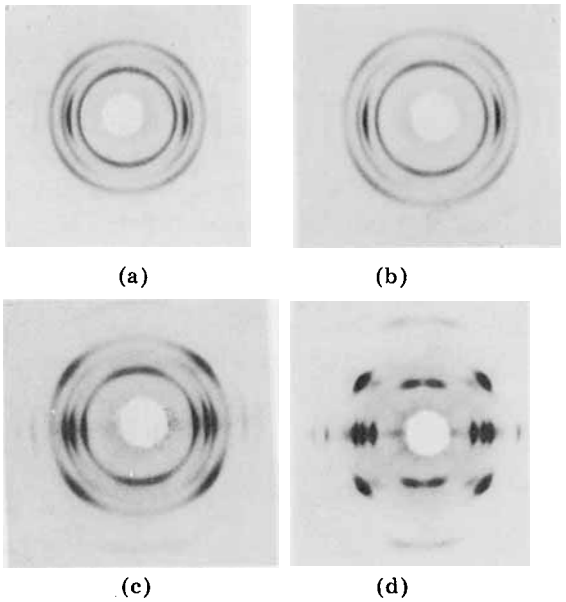

Fig. 5. Effect of molecular weight and extrusion rate on the WAXS patterns of samples spun at 200 m/min. Extrusion temperature is 230°C. Extrusion rate for (a), (b), and (c) is 2.1 g/min: (a) H-1200; (b) T-900; (c) T-0255; (d) H-0042 (extrusion rate is 0.5 g/min).

variables unchanged decreases the viscosity in the upper part of the threadline and results in lower orientation in the spun filament as shown in Figure 4 (compare also to Fig. 2.).

The effect of the molecular weight on the WAXS pattern is illustrated in Figure 5. Comparing the WAXS patterns in Figure 5(a)–5(c) for H-1200, T-900, and T-0255 at a melt extrusion rate of 2.1 g/min and take-up velocity 200 m/min, there seems to be a noticeable decrease in the 110 and 130 arc widths with increasing molecular weight indicating an increase of orientation.

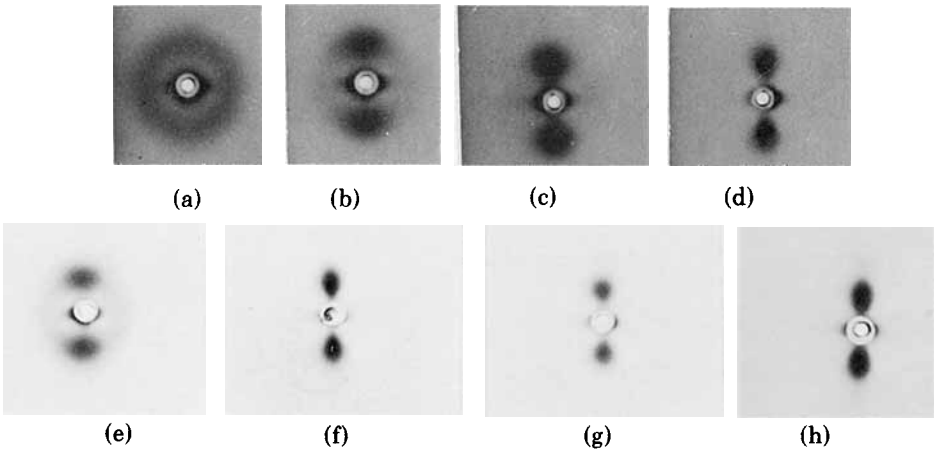

Fig. 6. SAXS patterns for melt-spun polypropylene filaments: (a) H-0660, T_E = 260°C, V_L = 50 m/min; (b) H-0660, T_E = 260°C, V_L = 300 m/min; (c) H-0660, T_E = 230°C, V_L = 300 m/min; (d) H-0660, T_E = 230°C, V_L = 550 m/min; (e) T-0255, T_E = 230°C, V_L = 50 m/min; (f) T-0255, T_E = 230°C, V_L = 200 m/min; (g) H-0042, T_E = 230°C, V_L = 50 m/min; (h) H-0042, T_E = 230°C, V_L = 200 m/min.

Comparison of the WAXS pattern for H-0042 sample (Fig. 5) with the other patterns in Figure 5 (spun at same take-up velocity but higher melt extrusion rate) indicates that this H-0042 sample has developed much higher levels of orientation than the other samples. This drastic difference in orientation appears to be a result of a combination of two effects: (1) low extrusion rate and (2) higher molecular weight. The lower extrusion rate results in a lower extrusion velocity through the spinneret capillary and, hence, a higher draw-down ratio (V_L/V_0) for a given take-up velocity. As noted in the previous section, this also leads to higher spinline stresses.

Figure 6 shows the SAXS patterns of various polypropylene filaments spun under a variety of conditions. Under conditions which give rise to low spinline

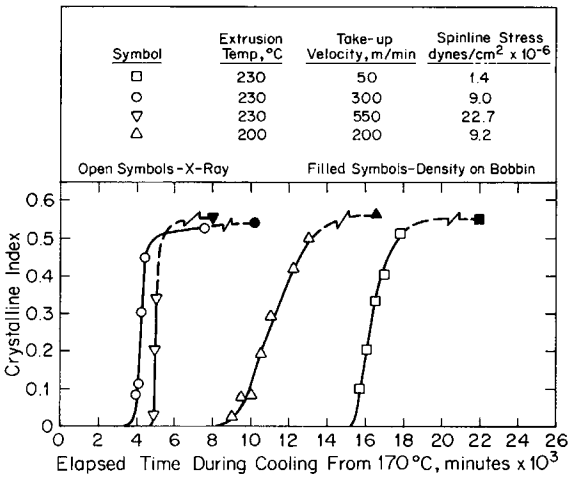

Fig. 7. Crystalline index as a function of residence time in the spinline from analysis of WAXS patterns. Polymer is H-0660 in all cases.

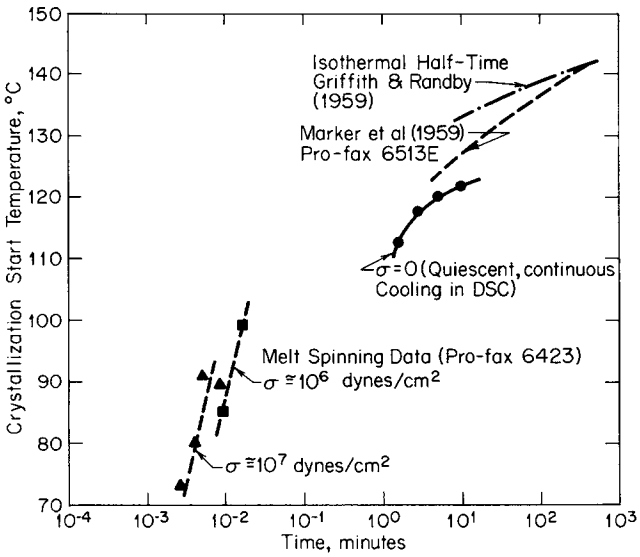

Fig. 8. CCT curve interpretation of crystallization kinetics as a function of cooling rate and stress.

stress such as low take-up velocity and high extrusion temperature, the small-angle pattern exhibits a continuous ring of nearly uniform intensity [Fig. 6(a)]. These are the same conditions which lead to low orientation in the WAXS pattern [Fig. 4(c)]. As the spinning conditions are changed so as to increase the spinline stress, the patterns evolve to definite "two-point" patterns [Fig. 6(b)–6(h)].

On-Line Crystallization Kinetics

Crystallinity levels were obtained from on-line WAXS patterns. These are plotted as a function of spinline residence time in Figure 7. These results generally show an increased rate of crystallization with increased take-up velocity or tension, other things being equal. However, because these are nonisothermal results, it is necessary to separate out the effects of cooling rate, which also increases with take-up velocity, from those due to stress.

These experimental results can be interpreted in terms of "continuous cooling transformation" curves utilized by metallurgists to interpret solid-phase transformations, especially heat treatment of steel.[36] This approach, previously discussed by Spruiell and White,[11,12] is illustrated in Figure 8. Decreased crystallization start temperatures are observed with increased cooling rate. The effect of stress is to shift the CCT curve to shorter times. A comparison is also shown in Figure 8 of the melt-spinning data to the isothermal crystallization data of Griffiths and Randby[37] and Marker et al.[38]

Crystallinity of Spun Fibers

Density measurements for the monoclinic filaments obtained by spinning in air were used to compute the per cent crystallinity in the samples. These measurements indicated crystallinities of order 55 ± 3% for all samples. Careful examination indicated a trend toward increased crystallinity with take-up ve-

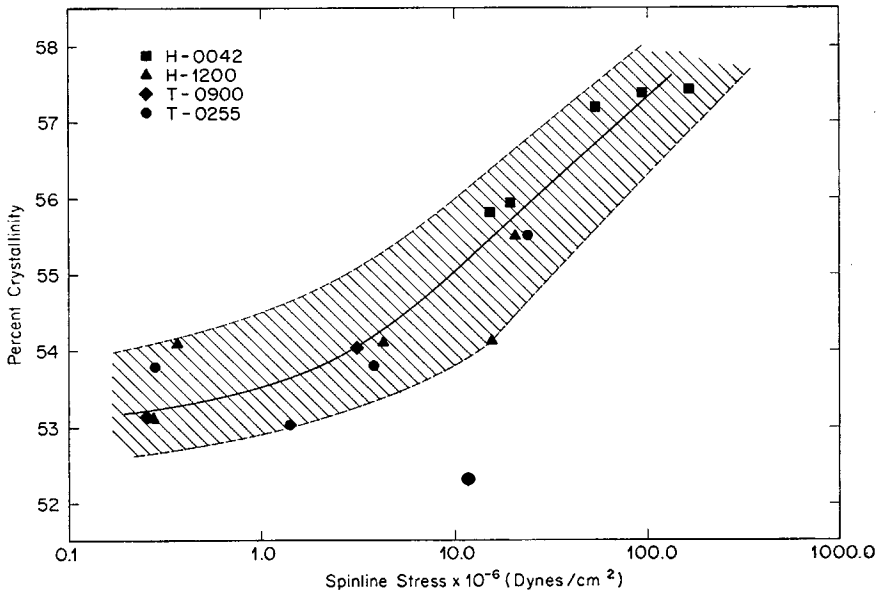

Fig. 9. Crystallinity level of melt-spun fibers as a function of spinline stress.

locity and take-up stress (see Fig. 9). Generally, the Hercules polypropylenes tend to have a slightly higher level of crystallinity than the Tennessee Eastman polymers.

Molecular Orientation

Figure 10 shows Hermans–Stein c-axis crystalline orientation factor (f_c) for the isotactic polypropylenes plotted against the take-up velocity. The orientation factor increases steadily with the take-up velocity. The figure also shows the effect of the molecular weight on the orientation factors. At any given take-up velocity, f_c was found to be higher for higher molecular weight samples. The effect of tacticity, if any, on f_c is not very clear from these results. The large effect of a combination of a higher draw down ratio and high molecular weight is exhibited by the H-0042 filaments. At take-up velocities of 200, 400, and 550 m/min, these filaments show very high values of f_c (~0.9).

Figure 11 shows crystalline orientation functions plotted versus the spinline stress for the various polypropylenes. Each of the orientation functions f_a, f_b, and f_c falls on a single curve within the experimental accuracy. This shows the importance of the spinline stress on the development of morphology during melt spinning. The value of f_c increases with spinline stress, leveling off at 0.91, which indicates that the c-axes are tending to become more aligned with the fiber axis with increasing stress. The b-axis orientation function (f_b) decreases rapidly reaching a value of −0.48, indicating a near-perpendicular alignment of the b-axes with the fiber axis. The value of $f_{a'}$ decreases slowly at first, but it then decreases rapidly as f_c rises and finally approaches −0.43.

Figure 12 presents the measured birefringence of the filaments as a function of spinline stress. These data were used to obtain the amorphous orientation factors. The amorphous orientation factors were computed from eq. (6) with

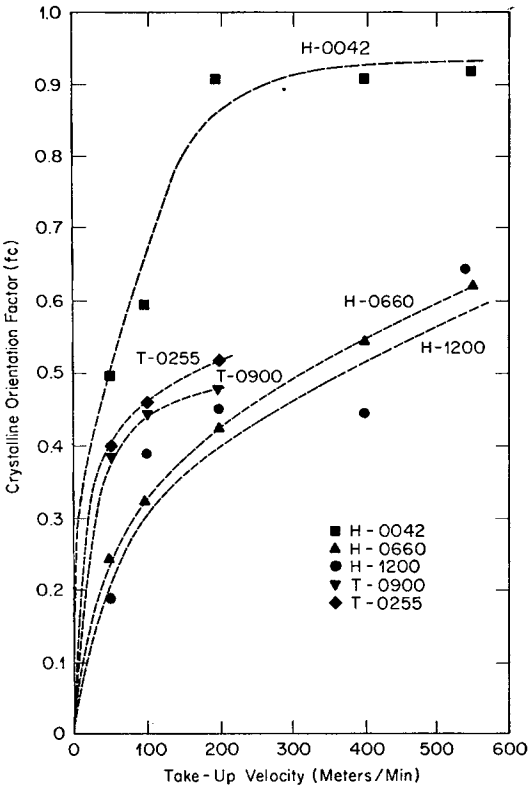

Fig. 10. Hermans–Stein c-axis orientation factor of spun fibers as a function of take-up velocity showing influence of molecular weight.

Δ_{form} taken equal to zero. Although both the crystalline and amorphous orientation factors increase with increasing spinline stress, the orientation developed in the amorphous chains is always much smaller than the orientation in the crystalline regions. The values of the amorphous orientation factors range from slightly less than zero up to about 0.3.

Discussion of Structure Development

The qualitative features of the present study are in general agreement with those of earlier researchers.[1,4–12] The filaments melt spun into water exhibited a paracrystalline, "smectic" structure, while those spun into ambient air were monoclinic. The crystallinity values of the latter samples were of the same order as those obtained by Sheehan and Cole[1] and Samuels.[17,33,34] Orientation increases with take-up velocity and melt draw-down in a way similar to that reported by Kitao et al.,[8] Henson,[10] and Spruiell and White.[11] The variation in the SAXS pattern from a ring pattern at low spinline stresses to a "two point" pattern at high spinning stresses is similar to the behavior reported by Noether and Whitney[4] and Spruiell and White.[11]

In general, the variations in crystalline orientation factors and SAXS patterns are qualitatively similar to those reported for high-density polyethylene.[8,12,21–23] Dees and Spruiell[22] have interpreted these features in the case of polyethylene

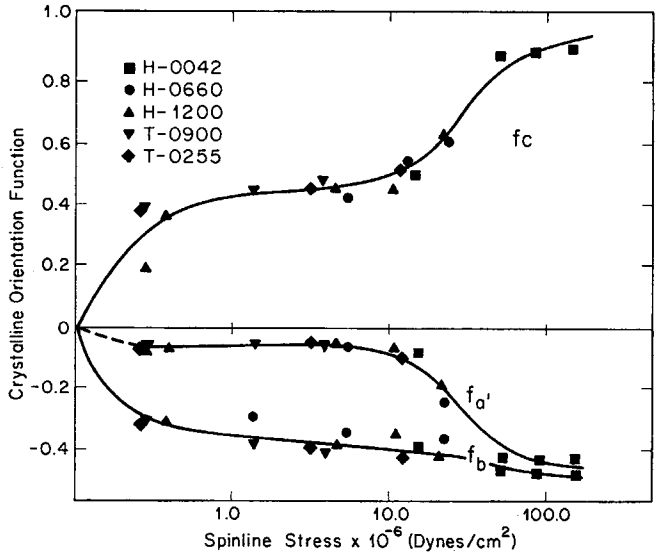

Fig. 11. Hermans–Stein *a*-, *b*-, and *c*-axis orientation factors of spun fibers as a function of spinline stress for five polypropylenes.

to indicate spherulitic morphology at very low spinning stresses which undergoes a transition to a row-nucleated[36] or cylindritic morphology as the spinning stress increases. Spruiell and White[11] have extended this interpretation to the case of polypropylene and the present data are certainly consistent with this general interpretation.

As pointed out by several investigators, polypropylene exhibits a distinctive bimodal orientation of the unit cells when crystallized from the melt under conditions of extensional flow.[9,18–20] Careful examination of the x-ray patterns shown in Figures 2–5 shows that this bimodal orientation occurs in our melt-spun filaments. The bimodal orientation is characterized by one component of the distribution with the *c*-(chain)axes parallel to the fiber axis and the second component with the *c*-axes approximately perpendicular to the fiber axis. The former component is here referred to as the *c*-axis-oriented population, while the latter is referred to as the *a'*-axis-oriented population. In the case of the H-0660 filaments, we have attempted to assess the relative contribution of these two components to the total orientation by separating the intensity distribution in the 110 reflection into components due to random, *a'*-axis-oriented, and *c*-axis-oriented crystals. The results are shown in Figure 13. It is clear that at high spinline stresses the largest proportion of the filament is in the *c*-axis-oriented population with only about 10–20% of the filament in the *a'*-axis-oriented population. The presence of the bimodal orientation is thus not likely to invalidate the broad qualitative features of the morphologic structure described in the preceding paragraph. The significance of the *a'*-axis-oriented component on the morphology of flow-crystallized polypropylene has been considered by Clark and Spruiell[20] and Anderson and Carr.[9] Both conclude that the secondary, or *a'*-axis-oriented, component consists of very small crystals distributed throughout the sample and probably growing with an epitaxial relationship to the primary, or *c*-axis-oriented, component.

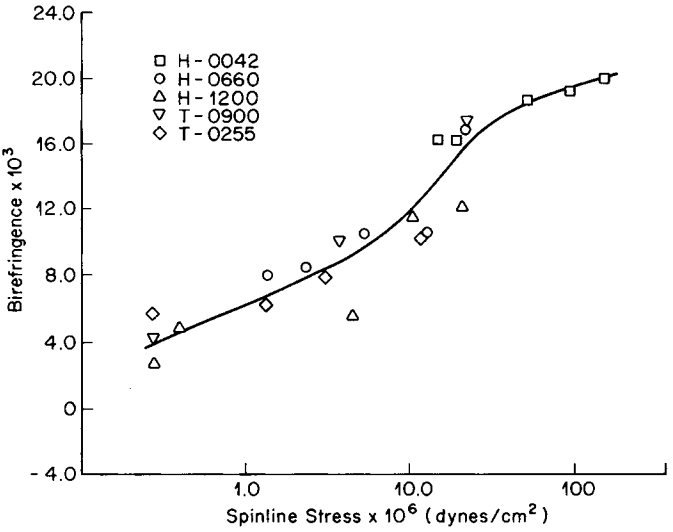

Fig. 12. Birefringence of spun fibers as a function of spinline stress.

A major finding of the present investigation is that the morphology of a broad range of polypropylenes over a range of spinning variables is largely determined by the spinline stress. Figures 9, 11, and 12, 11 in particular, attest to this fact. Spruiell and White[11] have previously published results indicating similar behavior for H-0660 spun at three different temperatures. We may conclude, therefore, that spinning variables such as polymer molecular weight, flow rate, melt temperature, and take-up velocity all affect the morphology of the spun filaments, but the combination of these effects on morphology can be traced to their effect on spinline stress. This result is reasonable if one considers that orientation and birefringence in polymer melts[39–41] and vulcanized rubber[42] are determined by stress and that the orientation of the amorphous phase just as crystallization begins probably determines the crystalline morphology.

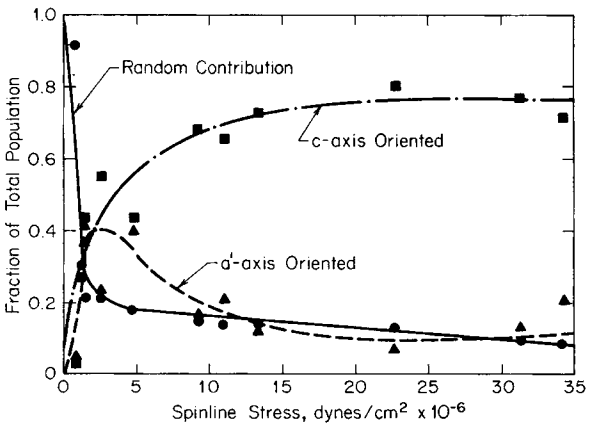

Fig. 13. Relative orientation contributions in H-0660 polypropylene filaments.

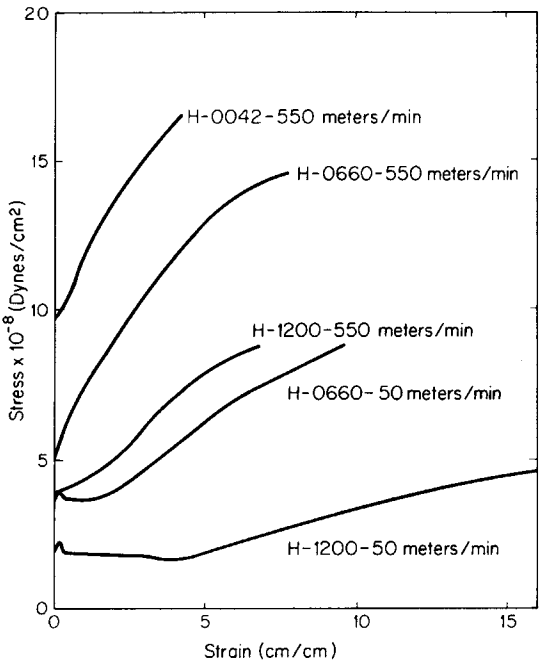

Fig. 14. Typical engineering stress vs strain curves for melt-spun polypropylene fibers.

MECHANICAL PROPERTIES OF SPUN FILAMENTS

Engineering stress (force/initial cross-sectional area)-versus-strain ($\Delta L/L_0$) curves computed from force-versus-elongation data are shown in Figure 14 for typical as-spun filaments. In general, tangent modulus, yield strength, and tensile strength increase with take-up velocity and molecular weight. Elongation to break exhibits the reverse trend. The tensile strength and elongation to break are shown as a function of take-up velocity in Figure 15. The plotted points in this figure and others presented later represent average values from several tests (usually five).

Another observation which can be made from Figure 14 is that filaments spun under low stress conditions exhibited a yield drop and necking elongation, while those spun under higher spinline stresses exhibited less prominent necking.

Figures 16 and 17 show modulus, yield strength, tensile strength, and per cent elongation to break plotted against the spinline stress. For all the samples, the modulus, yield strength, and tensile strength increase while the percent elongation decreases with the spinline stress. It is of interest that the tensile property results from samples of different molecular weights appear to lie within a scatter band which is hardly broader than the expected scatter for the data from a given molecular weight sample. That is, the data appear to be correlated together by the spinline stress.

DISCUSSION

That the mechanical properties may be correlated to the spinline stress evidently results from the fact that the structural features which control the me-

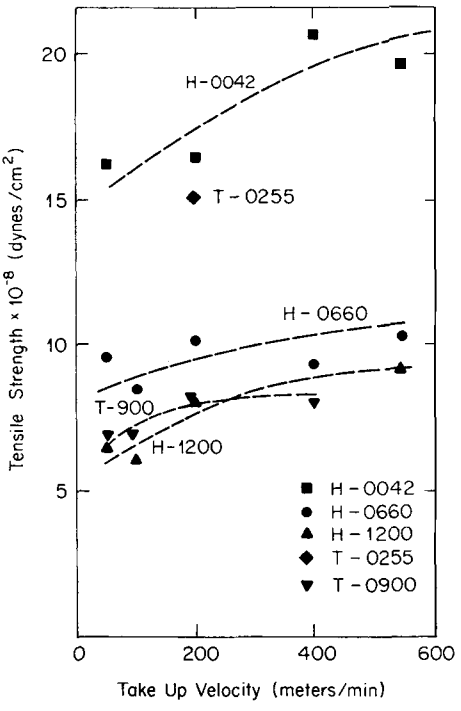

(a)

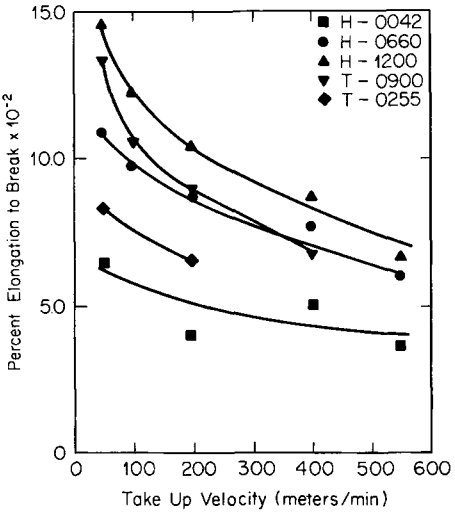

(b)

Fig. 15. (a) Tensile strength vs take-up velocity for as-spun polypropylene filaments. (b) Percent elongation to break vs take-up velocity for as-spun polypropylene filaments.

chanical properties are determined by the spinline stress. In the preceding section, it was shown that the molecular orientation and probably other morphologic features of the spun filaments are determined by the spinline stress. We have attempted to establish which features of the morphology are most important in determining the mechanical properties of our spun filaments by

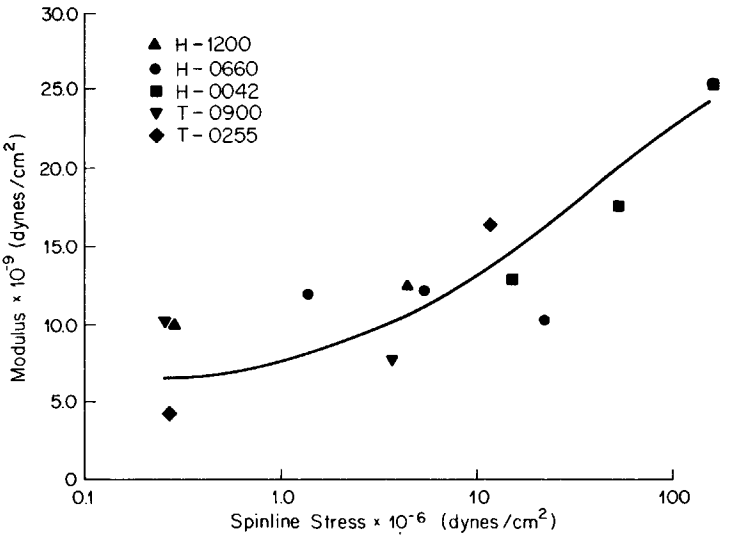

Fig. 16. (a) Young's (tangent) modulus vs spinline stress for polypropylene filaments. (b) Yield strength vs spinline stress for polypropylene filaments.

plotting the properties versus different measurable parameters such as c-axis crystalline orientation factor, amorphous orientation factor, and birefringence (a measure of average orientation). All such parameters correlate the mechanical properties to some degree. The correlation with these structural parameters seemed to produce slightly more scatter than in the case of the spinline stress. Within the range of variables studied, there was little difference between the correlations provided by these various parameters.

The authors would like to thank Hercules, Inc., and Tennessee Eastman for supplying the polymers of this study. Dr. P. Drechsel of Hercules was especially helpful in characterizing samples. This research was supported in part by the National Science Foundation under Grant GK-18897.

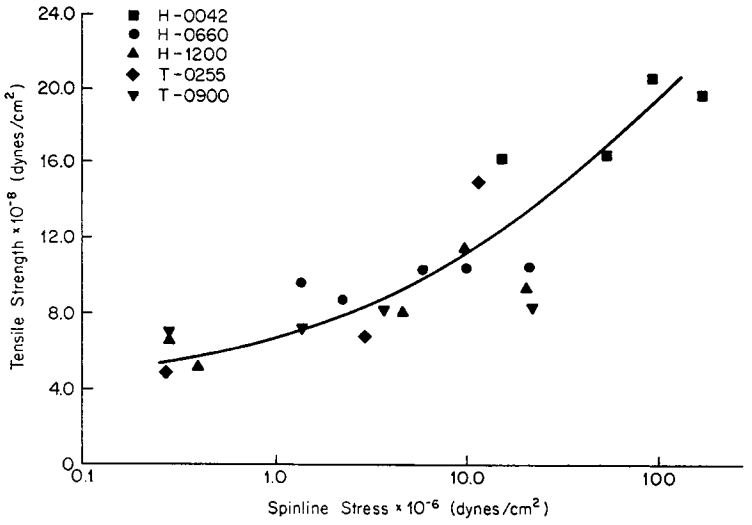

(a)

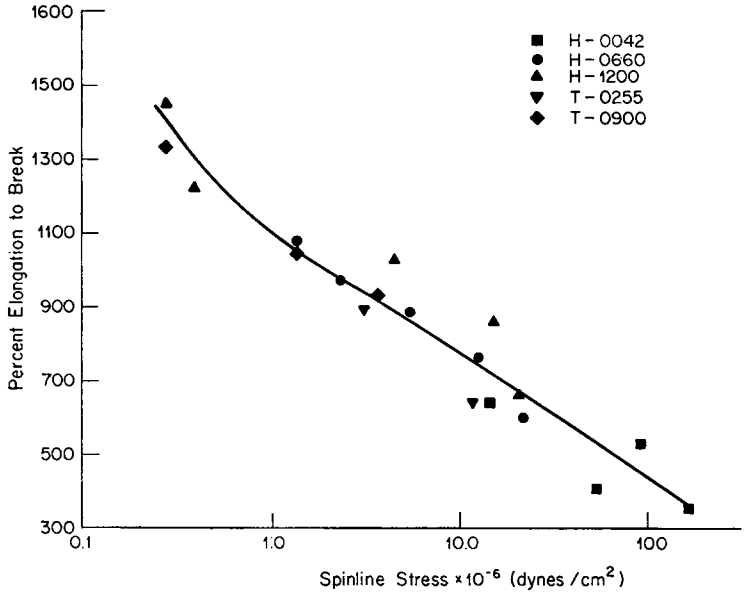

(b)

Fig. 17. (a) Tensile strength vs spinline stress for polypropylene filaments. (b) Percent elongation to break vs spinline stress for as-spun polypropylene filaments.

References

1. W. C. Sheehan and T. B. Cole, *J. Appl. Polym. Sci.*, **8**, 2359 (1964).
2. A. J. Herrman, U.S. Pat. 3,256,258 (1966); Br. Pat. 935,809 (1963).
3. E. S. Clark in *Structure and Properties of Polymer Films*, R. W. Lenz and R. S. Stein, Eds., Plenum, New York, 1972.
4. H. D. Noether and W. Whitney, *Kolloid Z. Z. Polym.*, **251**, 991 (1973).
5. B. S. Sprague, *J. Macromol. Sci.-Phys.*, **B8**, 157 (1973).
6. K. Katayama, T. Amano, and K. Nakamura, *Kolloid Z. Z. Polym.*, **226**, 125 (1968).
7. P. Y-F. Fung, E. Orlando, and S. H. Carr, *Polym. Eng. Sci.*, **13**, 295 (1973).

8. T. Kitao, S. Ohya, J. Furukawa, and S. Yamashita, *J. Polym. Sci.*, **11,** 1091 (1973).
9. P. G. Anderson and S. H. Carr, *J. Mater. Sci.*, **10,** 870 (1975).
10. H. M. Henson and J. E. Spruiell, paper presented at Division of Cellulose, Paper and Textile Chemistry, American Chemical Society, Philadelphia, April 1975.
11. J. E. Spruiell and J. L. White, *Polym. Eng. Sci.*, **15,** 660 (1975).
12. J. E. Spruiell and J. L. White, in *Fiber and Yarn Processing*, J. L. White, Ed., *Appl. Polym. Symp.*, **27,** 121 (1975).
13. O. Ishizuka and K. Koyama, *Sen-i-Gakkaishi,* **32,** T-43 (1976).
14. J. J. Hermans, P. H. Hermans, D. Vermeas, and A. Weidinger, *Rec. Trav. Chim. Pays-Bas,* **65,** 427 (1946).
15. R. S. Stein, *J. Polym. Sci.*, **31,** 327 (1958).
16. Z. W. Wilchinsky, *J. Appl. Phys.*, **30,** 792 (1959); *ibid.*, **31,** 1969 (1960); *Adv. X-Ray Anal.*, **6,** 231 (1963).
17. R. J. Samuels, *Structured Polymer Properties*, Wiley-Interscience, New York, 1974.
18. M. Compostella, A. Coen, and F. Bertinotti, *Angew. Chem.*, **74,** 618 (1962).
19. E. S. Clark, *Bull. Amer. Phys. Soc.*, March 1970.
20. E. S. Clark and J. E. Spruiell, *Polym. Eng. Sci.*, **16,** 176 (1976).
21. L. E. Abbott and J. L. White, in *U.S.-Japan Seminar on Polymer Processing and Rheology,* C. D. Bogue, M. Yamamoto, and J. L. White, Eds., *Appl. Polym. Symp.*, **20,** 247 (1973).
22. J. R. Dees and J. E. Spruiell, *J. Appl. Polym. Sci.*, **18,** 1053 (1974).
23. J. L. White, K. C. Dharod, and E. S. Clark, *J. Appl. Polym. Sci.*, **18,** 2539 (1974).
24. V. G. Bankar, J. E. Spruiell, and J. L. White, Melt Spinning of Nylon-6: Structure Development and Mechanical Properties of As-Spun Filaments, University of Tennessee, Polymer Science and Engineering Rep. No. 64, July 1976, *J. Appl. Polym. Sci.* (to appear).
25. R. Chaing, *J. Polym. Sci.*, **28,** 235 (1958).
26. J. P. Tordella, in *Rheology,* Vol. 5, F. R. Eirich, Ed., Academic Press, New York, 1969.
27. J. L. White, in *U.S.-Japan Seminar on Polymer Processing and Rheology,* D. C. Bogue, M. Yamamoto, and J. L. White, Eds., *Appl. Polym. Symp.*, **20,** 155 (1973).
28. G. Natta and P. Corradini, *Nuovo Cimento Suppl.*, **15,** 40 (1960).
29. L. H. Tung and W. C. Taylor, *J. Polym. Sci.*, **21,** 144 (1956).
30. F. Danusso, G. Moraglio, W. Ghiglia, L. Motta, and G. Talamini, *Chim. Ind.*, **41,** 748 (1959).
31. R. S. Stein and F. H. Norris, *J. Polym. Sci.*, **21,** 381 (1956).
32. S. Hoshino, J. Powers, D. G. Legrand, H. Kawai, and R. S. Stein, *J. Polym. Sci.*, **58,** 185 (1962).
33. R. J. Samuels, *J. Polym. Sci. A-2,* **6,** 2021 (1968).
34. R. J. Samuels, *J. Macromol. Sci. Phys.*, **B4,** 701 (1970).
35. M. Born and E. Wolf, *Principles of Optics,* 4th ed., Pergamon, Oxford, 1970.
36. A. Keller and M. Machin, *J. Macromol. Sci. Phy.*, **B1,** 41 (1967).
37. J. H. Griffiths and B. G. Randby, *J. Polym. Sci.*, **38,** 107 (1959).
38. L. Marker, P. M. Hay, G. P. Tilley, R. M. Early, and O. J. Sweeting, *J. Polym. Sci.*, **38,** 33 (1959).
39. W. Philippoff, *J. Appl. Phys.*, **27,** 984 (1956).
40. A. S. Lodge, *Trans. Faraday Soc.*, **52,** 120 (1956).
41. E. B. Adams, J. C. Whitehead, and D. C. Bogue, *A.I.Ch.E.J.*, **11,** 1026 (1965).
42. L. R. G. Treloar, *Physics of Rubber Elasticity,* 2nd ed., Oxford (1958).

Received August 6, 1976
Revised October 14, 1976